



**HAL**  
open science

## Common structural requirements for heptahelical domain function in class A and class C G protein-coupled receptors.

Virginie Binet, Béatrice Duthey, Jennifer Lecaillon, Claire Vol, Julie Quoyer, Gilles Labesse, Jean-Philippe Pin, Laurent Prézeau

### ► To cite this version:

Virginie Binet, Béatrice Duthey, Jennifer Lecaillon, Claire Vol, Julie Quoyer, et al.. Common structural requirements for heptahelical domain function in class A and class C G protein-coupled receptors.. *Journal of Biological Chemistry*, 2007, 282 (16), pp.12154-63. 10.1074/jbc.M611071200 . inserm-00318820

**HAL Id: inserm-00318820**

**<https://inserm.hal.science/inserm-00318820>**

Submitted on 5 Sep 2008

**HAL** is a multi-disciplinary open access archive for the deposit and dissemination of scientific research documents, whether they are published or not. The documents may come from teaching and research institutions in France or abroad, or from public or private research centers.

L'archive ouverte pluridisciplinaire **HAL**, est destinée au dépôt et à la diffusion de documents scientifiques de niveau recherche, publiés ou non, émanant des établissements d'enseignement et de recherche français ou étrangers, des laboratoires publics ou privés.

# COMMON STRUCTURAL REQUIREMENTS FOR HEPTAHELICAL DOMAIN FUNCTION IN CLASS A AND CLASS C GPCRS

Virginie Binet<sup>1,2</sup>, Béatrice Duthey<sup>1</sup>, Jennifer Lecaillon<sup>1</sup>, Claire Vol<sup>1</sup>, Julie Quoyer<sup>1</sup>, Gilles Labesse<sup>3</sup>, Jean-Philippe Pin<sup>1</sup> and Laurent Prézeau<sup>1</sup>

From<sup>1</sup> CNRS-UMR 5203, Montpellier, France; INSERM-U661, Montpellier, France; Univ. Montpellier 1, Montpellier, France; Univ. Montpellier 2, Montpellier, France; IGF (Institut de Génomique Fonctionnelle), Department of Molecular Pharmacology, Montpellier, France,<sup>2</sup> Centre Hospitalo-Universitaire de Montpellier, Montpellier, France;<sup>3</sup> Centre de Biochimie Structurale, CNRS UMR 5048 Montpellier, France; INSERM U554, Montpellier, France; Univ. Montpellier 1, Montpellier, France; Univ. Montpellier 2, Montpellier, France.

Running Title: Ionic lock involving TM3 and TM6 in a class C receptor

Address correspondence to: Laurent Prézeau, Département de Pharmacologie Moléculaire, Institut de Génomique Fonctionnelle, 141 rue de la Cardonille, 34094 Montpellier cedex 5. Tel.: +33 (0)467 14 29 33 ; Fax : +33 (0) 467 54 24 32 ; email : [laurent.prezeau@igf.cnrs.fr](mailto:laurent.prezeau@igf.cnrs.fr)

**G protein-coupled receptors (GPCRs) are key players in cell communication. Several classes of such receptors have been identified. Although all GPCRs possess a heptahelical domain directly activating G proteins, important structural and sequence differences within receptors from different classes suggested distinct activation mechanisms. Here we show that highly conserved charged residues likely involved in an interaction network between transmembrane domains (TM) 3 and 6 at the cytoplasmic side of class C GPCRs are critical for activation of the GABA<sub>B</sub> receptor. Indeed, the loss of function resulting from the mutation of the conserved lysine residue into aspartate or glutamate in the TM3 of GABA<sub>B2</sub> can be partly rescued by mutating the conserved acidic residue of TM6 into either lysine or arginine. In addition, mutation of the conserved lysine into an acidic residue leads to a non-functional receptor that displays a high agonist affinity. This is reminiscent to a similar ionic network that constitutes a lock stabilizing the inactive state of many class A rhodopsin-like GPCRs. These data reveal that despite their original structure class C GPCRs share with class A receptors at least some common structural feature controlling G-protein activation.**

G-protein coupled receptors (GPCRs) are encoded by one of the most important gene families in mammalian genomes (1). These membrane proteins play a critical role in transducing extracellular signals into the cell, and constitute the major target for drug development.

Although being important molecules, still little is known about their activation mechanism (2,3). All these receptors possess a heptahelical domain (HD), the structure of which has been solved for rhodopsin only (4). This available structure is in a fully inactive state, as it is stabilized by the covalently linked inverse agonist cis-retinal. Thus, our actual knowledge on the active conformation relies mostly on functional and biophysical analysis of a variety of mutated receptors and their coupling to G proteins and their effectors (2,3).

Four main classes of GPCRs have been defined in mammals based on sequence analysis ((1,5,6) and <http://www.gpcr.org/7tm/>), the rhodopsin-like class A receptors being the largest and the most studied one. Class A receptor activation is associated with a movement of TM6 relative to TM3, leading to the opening of a cavity between the intracellular loops 2 and 3 connecting TM3 to TM4, and TM5 to TM6, respectively (2,7). The inactive state is stabilized by a network of interactions between residues at the cytoplasmic end of the TMs (4). This network includes ionic interactions that involve the highly conserved class A residues D/ERY at the cytoplasmic end of TM3. In many class A GPCRs, the Arg of the D/ERY motif makes an ionic interaction with a conserved acidic residue (D/E) of TM6 (3). Mutation of these residues leads either to a loss or a gain of function, consistent with this motif being involved in a lock that can control the conformational state of class A GPCRs (3,8,9). Alternatively, the Arg of the D/ERY motif has also been proposed to play a direct role in receptor G-protein interaction and activation for some class A receptors (8).

The D/ERY motif is not found in the GPCRs from the other classes. This is the case for the class C receptors which are activated by the two main neurotransmitters, glutamate and  $\gamma$ -aminobutyrate (GABA), by  $\text{Ca}^{2+}$  ions, taste compounds and pheromones (10). The sequence divergence between the HDs of class A and class C GPCRs questioned whether both get activated the same way. In addition, class C receptor general functioning appears quite different from that of class A receptors despite their likely common dimeric organization (11). Whereas conformational changes within the HD of Class A GPCRs is regarded as the main step in receptor activation, activation of Class C receptors is assumed to result from a change in the relative position of the subunits in the dimer. Indeed, the crystal structure of the large dimeric extracellular domain (ECD) of mGlu1 with and without bound agonist, revealed a major change in their relative position resulting from agonist binding (12). Moreover, FRET analysis in living cells with CFP and YFP fused at various places in the intracellular segments of each of the subunits is consistent with a relative movement of the HDs during class C receptor dimer activation (13). However, a number of modeling and mutagenesis studies are consistent with the HDs of class C GPCRs being structurally similar to rhodopsin (10,14,15). Thus, besides the putative movement between the HDs (13), a change in the conformation of the HDs themselves is likely also involved, as indicated by the effect of allosteric regulators interacting directly in the HD (15-18). But are any of the structural requirements involved in such a conformational change similar in both class A and class C GPCRs?

In the present study, we aimed at identifying key residues involved in the activation of class C GPCRs. Using the  $\text{GABA}_B$  receptor as a model system, we thus examined the functional consequences resulting from the mutation of such residues. This leads us to the observation that a network of interactions involving TM3 and TM6 plays a critical role in the activation process, illustrating some similarity in the structural determinants controlling G-protein activation by class A and class C GPCRs.

#### Experimental procedures

*Materials* - GABA was purchased from Sigma (L'Isle d'Abeau, France).  $^3\text{H}$ -CGP54626 purchased from Tocris (Tocris, Bristol, UK) had a specific activity of  $40 \text{ Ci}\cdot\text{mmol}^{-1}$ . CGP54626 was purchased from Tocris (Fisher-Bioblock, Illkirch,

France). Fetal bovine serum (FBS), culture media and other solutions used for cell culture were from GIBCO-BRL-Life Technologies, Inc. (Cergy Pontoise, France). [ $^3\text{H}$ ]-myo-inositol ( $23.4 \text{ Ci/mol}$ ) was purchased from Perkin-Elmer Life Science (NEN) (Paris, France). All other reagents used were of molecular or analytical grade where appropriate.

*Plasmids and site-directed mutagenesis* - The plasmids encoding the wild-type and chimeric  $\text{GABA}_{B1a}$  and  $\text{GABA}_{B2}$  subunits epitope tagged at their N-terminal ends (pRK- $\text{GABA}_{B1a}$ -HA, pRK- $\text{GABA}_{B2}$ -cMyc), under the control of a CMV promoter, were previously described (19,20). Site-directed mutagenesis was performed on a pRK- $\text{GABA}_{B1a}$ -HA or a pRK- $\text{GABA}_{B2}$ -cMyc vector using a Quick-Change® strategy (Stratagene). Briefly, the mutations were generated by using two complementary 30- to 40-mer oligonucleotides designed to contain the desired mutation and the sequence of the constructs was confirmed by DNA sequencing (Genome Express, France).

*Cell culture and transfection* - Human embryonic kidney (HEK) 293 cells were cultured in Dulbecco's modified Eagle's medium supplemented with 10% FCS and transfected by electroporation as described elsewhere (17). Unless stated otherwise,  $10^7$  cells were transfected with plasmid DNA containing the coding sequence of the receptor subunits, and completed to a total amount of  $10 \mu\text{g}$  plasmid DNA with pRK $_6$  plasmid. For determination of inositol phosphate accumulation, the cells were also transfected with the chimeric Gaq1 G-protein which allows the coupling of the recombinant heteromeric  $\text{GABA}_B$  receptor to PLC (20).

*Measurement of inositol phosphate production* - Determination of inositol phosphate (InP) accumulation in transfected cells was performed in 96-wells plates ( $0.2 \times 10^6$  cells/well) after over-night labeling with  $^3\text{H}$ -myo-inositols ( $0.5 \mu\text{Ci/well}$ ) as already described (21). The stimulation was conducted for 30 minutes in a medium containing 10mM LiCl and the indicated concentration of agonist or antagonist. The reaction was stopped by replacing the medium by 0.1M formic acid. Supernatants were recovered and InP were purified by ion exchange chromatography using DOWEX AG1-X8 resin (Biorad, Marnes-la-Coquette, France) in 96 well filter plates (Millipore, Bedford, MA). Total radioactivity remaining in the membrane fractions was counted after treatment of cells with a solution containing 10% triton X-100 and 0.1N NaOH. Radioactivity was quantified using Wallac 1450

MicroBeta liquid scintillation counter. Data were expressed as the amount of total InPs produced over the amount of radioactivity remaining in the membranes plus the produced InP, multiplied by 100. Unless stated otherwise, all data are means  $\pm$  sem of at least 3 independent experiments. The dose-response curves were fitted using the GraphPad (San Diego) PRISM software and the following equation " $y = [(y_{\max} - y_{\min}) / (1 + (x/EC_{50})^{nH})] + y_{\min}$ " where the  $EC_{50}$  is the concentration of the compound necessary to obtain 50% of the maximal effect and  $nH$  is the Hill coefficient.

*Anti HA tag ELISA for quantification of cell surface expression* - Twenty four hours after transfection ( $10^7$  cells, HA-tagged GABA<sub>B1</sub> (2 $\mu$ g) and cMyc-tagged GABA<sub>B2</sub> (2 $\mu$ g) subunits), cells were fixed with 4% paraformaldehyde and then blocked with PBS + 5% FBS. After 30 minutes reaction with primary antibody (monoclonal anti-HA clone 3F10 (Roche, Basel, Switzerland) at 0.5 $\mu$ g/mL) in the same buffer, the goat Anti-Rat antibody coupled to horseradish peroxidase (Jackson ImmunoResearch, West Grove, PA) was applied for 30 minutes at 1 $\mu$ g/mL. After intense washes with PBS, secondary antibody was detected and quantified instantaneously by chemiluminescence using Supersignal® ELISA femto maximum sensitivity substrate (Pierce, Rockford, IL) and a Wallac Victor<sup>2</sup> luminescence counter.

*Ligand binding on intact HEK293 cells* - Ligand binding experiments were performed on intact HEK293 cells. The cells were plated after electroporation the day before experiment. Thus, the cells on ice were washed with ice-cold binding buffer (20mM Tris-HL, pH7.4, 118mM NaCl, 1.2 mM KH<sub>2</sub>PO<sub>4</sub>, 1.2 mM MgSO<sub>4</sub>, 4.7 mM KCl, 1.8 mM CaCl<sub>2</sub>) and incubated in presence of 1.5 nM of <sup>3</sup>H-CGP54626 with or without unlabeled ligand at the indicated concentration. The incubation was terminated by washing with ice-cold binding buffer. The cells were disrupted with 0.1N NaOH (400mL) and the bound radioactivity was counted in a scintillation beta counter. Displacement curves were fitted with the GraphPad (San Diego) PRISM software, using the equation  $y = ((y_{\max} - y_{\min}) / (1 + (x/EC_{50})^{nH})) + y_{\min}$ , where  $EC_{50}$  is the concentration of cold drug necessary to displace half of the specially bound <sup>3</sup>H-CGP54626, and  $nH$  is the Hill number.

*Structural Biology* - Sequence alignment of Class C receptors was performed using Clustal W (22) and refined manually. Fold-compatibility for truncated sequences corresponding to the HD of various Class C receptors was searched using the meta-server @TOME (23), and Ref therein).

Sequence-structure alignments including various Class C receptors and the crystal structures of rhodopsin (PDB1LH9, PDB1U19 and PDB1GZM, (4,24,25)) were manually refined with the help of the program ViTO (26). Models of various receptors (mainly mGluRs, T1R2, T1R3, GABA<sub>B1</sub> and GABA<sub>B2</sub>) were performed using SCWRL3.0 (27) and MODELLER7.7 (28). In absence of tools for structure evaluation of modelled membrane proteins, several rounds of alignment refinement / molecular modelling were performed. Visual inspection of the localization of hydrophobic and/or conserved residues relative to the membrane interface and protein core was performed for each TM helix and then for the whole HD. Strict conservation was computed for each sub-family of Class C receptors (e.g.: GABA<sub>B2</sub>) or for the whole superfamily using ViTO. Final three-dimensional models were built for using MODELLER 7.7 with the loop optimization procedure.

## RESULTS

*Identification of conserved residues at the cytoplasmic ends of TM3 and TM6 of class C GPCRs*

Alignment of the sequences of class C receptor HDs revealed several highly conserved residues. Among these are two basic residues located at the cytoplasmic side of TM3, at positions close to that of the D/ERY motif in class A receptors (Fig.1). A second highly conserved position is that of an acidic residue of the cytoplasmic end of TM6 (Fig. 1).

In order to get some possible information on the functional role of these conserved charged residues, 3D models of class C HDs were generated based on rhodopsin structure (see <http://www.infobiosud.cnrs.fr/bioserver/HDC/suppl.html>). A fold-recognition approach using the meta server @TOME (<http://bioserv.cnrs.fr>) confirmed the expected compatibility of sequences from Class C receptors with the seven-helix bundle of rhodopsin and provided us with a structural alignment. However, due to the rather low level of sequence identity (~12%) this alignment needed to be refined and critically assessed. The alignment was refined taking into account: first the position of the highly conserved residues, considering these are likely buried in the core structure (Fig.2A); second, the position of the hydrophobic residues likely exposed to the plasma membrane; third, amino acid hydrophobicity was also used to delimitate helix termini, and large sequence variation (in length and amino acid

composition) was clustered in loops. The refinement of the combined alignment was performed by several rounds of manual editing, molecular modeling and structure analysis using the program ViTO on the @TOME meta-server. This strategy was first applied locally, i.e. on each TM separately, and then validated on the full model.

As illustrated with the GABA<sub>B2</sub> HD (Fig.2), the final models obtained for various Class C GPCR HDs, revealed consistencies with a rhodopsin-like structure. For example, TM 1 showed only a thin patch of conserved residues in agreement with its thin interhelical surface. Also in agreement with TM3 being mostly buried in the core structure, this helix showed the same bias in amino acid composition (enrichment in Ser, Thr, Gly and Ala) in class A and class C GPCRs. Moreover, the conserved disulphide bridge that links TM3 to TM5 in class A receptor is predicted to be present in class C GPCRs.

The final model obtained is in agreement with those already reported (14,29-33). Indeed an identical alignment of TM1, TM3, TM6, and TM7 with rhodopsin was even published for the Calcium Sensing receptor (33). These models were validated by directed mutagenesis of allosteric ligand putative binding sites. Indeed, the HD of Class C receptors contains a binding site for allosteric modulators at positions similar to that of the binding site of small ligands interacting with class A receptors (14,29-33). We further checked that our structural alignment is compatible with these additional restraints by building models for the corresponding receptors (especially GABA<sub>B2</sub>, mGluR1, mGluR5, CaSR and T1R3) and assessing the positions of the residues proposed to line the binding pocket (data not shown).

Using this alignment and the GABA<sub>B2</sub> model, we examined the predicted position of the highly conserved residues identified at the cytoplasmic face of TM3 and TM6 of class C GPCRs. The conserved arginine in TM3 (R575 in GABA<sub>B2</sub>) is shifted by one residue from the arginine of the D/ERY motif of class A receptors. However, it is optimally located near the solvent interface where the G proteins are expected to bind. Our model also places the conserved TM3 lysine (K572 in GABA<sub>B2</sub>) one helical turn above the former arginine in a buried and rather hydrophobic environment. Searching for negatively charged residues in the vicinity of this lysine highlighted solely the highly conserved aspartate of TM6 (D688 in GABA<sub>B2</sub>). Of interest, this aspartate residue is located one turn of alpha helix above the highly conserved acidic residue at the bottom of

TM6 in class A receptors (E247 in Rhodopsin). As depicted in Fig.2B, the 3D model of the class C GABA<sub>B2</sub> HD is consistent with the conserved charged residues identified in TM3 and TM6 facing each other. This ménage-à-trois might be involved in a network of ionic interactions mimicking that observed in class A GPCRs involving the D/ERY motif.

#### *Mutated GABA<sub>B</sub> subunits are correctly expressed at the cell surface*

To test the possible involvement of the conserved basic and acidic residues, these were mutated such that the charge is suppressed (alanine), conserved or inverted. To perform this study, we used the GABA<sub>B</sub> receptor as a model system. This receptor is a heterodimer composed of two homologous proteins GABA<sub>B1</sub> and GABA<sub>B2</sub>. Whereas the GABA<sub>B1</sub> subunit is responsible for agonist binding (34,35), the GABA<sub>B2</sub> subunit plays a pivotal role in G-protein activation (20,36-38). Of interest, one of the three conserved residues (arginine) is not conserved in the mammalian GABA<sub>B1</sub> HD (Fig. 1). As such, analyzing the role of these conserved residues in this receptor heterodimer may also allow a better understanding of the specific role of each HDs in G-protein activation.

We first mutated these three conserved residues (K572, R575 and D688) in the GABA<sub>B2</sub> subunit and co-expressed these with the wild-type GABA<sub>B1</sub> subunit. As shown in Fig. 3A, the mutated GABA<sub>B2</sub> subunits allow the correct surface targeting of the N-terminal HA-tagged GABA<sub>B1</sub> subunit (between 77±1% and 125±11% of the wild-type GABA<sub>B</sub> receptor cell surface expression), as revealed by an ELISA assay performed on intact cells using anti-HA antibodies. Because it is well known that GABA<sub>B1</sub> reaches the cell surface when associated with GABA<sub>B2</sub> only (19,39-41), these data indicate that the mutations introduced in the GABA<sub>B2</sub> HD affect neither GABA<sub>B2</sub> expression, nor its ability to form heterodimeric complexes with GABA<sub>B1</sub>.

Mutations of the corresponding residues in GABA<sub>B1</sub> (K683, W686, D800) were also generated. These HA-tagged mutants were expressed between 33±3% and 107±28% of the wild-type GABA<sub>B</sub> receptor (Fig. 4A) when co-expressed with GABA<sub>B2</sub>. Again, these data indicate that the mutations introduced in the HD of GABA<sub>B1</sub> do not restrict protein expression, nor the correct interaction of the mutant with GABA<sub>B2</sub> since interaction is needed for these subunits to reach the cell surface.

As expected by the modular nature of the GABA<sub>B</sub> heterodimeric receptor, all these mutant dimers were found to bind GABA at the surface of intact cells, as revealed by displacement of bound [<sup>3</sup>H]-CGP54626 by 1 mM GABA (data not shown).

*Mutation of the residues K572, R575 and D688 of GABA<sub>B2</sub> led to different phenotypes*

As shown in Fig.3B, the mutations of the three residues K572, R575, and D688 in GABA<sub>B2</sub>, led to different effects on the activity of the GABA<sub>B</sub> receptor as measured with an InP accumulation assay. Since the GABA<sub>B</sub> receptor is coupled to Gi/o G proteins, the GABA<sub>B</sub> subunits were co-transfected with the chimeric G protein Gqi9 allowing it to activate phospholipase C (42). As previously reported, this approach allowed the measurement of both basal and agonist-induced activities of the receptor (Fig.3B). As shown in Fig.3B, the mutation of R575 into any of the tested residues (R575K, R575A, R575D, R575E) suppressed GABA<sub>B</sub> receptor activity (both basal and agonist-stimulated). In contrast, the mutation of D688 into either alanine (D688A), lysine (D688K), arginine (D688R), or glutamate (D688E) led to a functional receptor, the D688E mutant displaying a higher constitutive activity than the wild-type (209±24% of wt basal activity) and a slightly higher agonist potency (EC<sub>50</sub> = 310±70 nM and 190±10 nM for the wild-type and the D688E mutant, respectively) (Fig.7). The D688R and D688K mutants are less active, with both a lower agonist-induced response and a lower basal activity (Fig.3B), and a GABA potency similar to or lower than that of the wild-type receptor (EC<sub>50</sub> = 640±160 and 410±80 nM for the D688K and D688R mutant respectively (Fig.7)).

In respect to the K572, its mutation into an acidic residue (K572D and K572E) suppressed receptor activity (both basal and agonist-induced, Fig.3B) despite the good expression level of these mutant subunits (124±22%, and 105±15% of wild-type expression, respectively, Fig.3A) and their ability to bind GABA (Fig. 8). This indicates that a negative charge at this position prevents GABA<sub>B</sub> receptor function. The mutation of this residue into either alanine or arginine led to functional receptors with lower basal (K572A) and agonist-induced (K572A and K572R) activities than the wild-type combination.

The mutation of the corresponding residues in GABA<sub>B1</sub> did not affect the functional properties of the GABA<sub>B</sub> receptor (Fig.4B; GABA EC<sub>50</sub> being 310±70, 490±60 and 640±100 nM for the wild-

type, GB1K683D and GB1D800K mutants, respectively).

*Inversion of the charge of D688 can rescue the function of the inactive K572D or K572E mutants*

The proposed model for the HD of GABA<sub>B2</sub> suggested that K572 and R575 of TM3 are facing D688 of TM6 suggesting the possible formation of an ionic interaction between TM3 and TM6. Therefore, we examined whether the mutation of D688 into either lysine or arginine could rescue the loss of function of the K572D, K572E, R575D or R575E mutants.

As shown in Fig.5A, receptors carrying the double mutations K572D-D688K, K572E-D688K, K572D-D688R, and K572E-D688R were all expressed at the cell surface like the wild-type receptor. Of interest, these four mutants could activate Gqi9 upon stimulation with saturating concentrations of GABA, although the responses measured were low compared to those obtained with the wild-type receptor (Fig.5B). The best responses were obtained with the K572D-D688K and the K572E-D688R mutants. Full dose-response curves of GABA further revealed that the lower response resulted from a lower coupling efficacy, rather than a large decrease in agonists potency (Fig.7). Indeed, the potency of GABA on K572D-D688K mutated receptor was only 3 fold lower than that measured on the wild-type receptor (EC<sub>50</sub> = 880±70 and 310±70 nM, respectively).

In contrast, mutating D688 into a basic residue did not restore function of the R575D and R575E mutants (Fig.6B), even though these double mutants were all found at the cell surface (Fig.6A).

These data highlight that opposite charges at positions 572 of TM3 and 688 of TM6 of GABA<sub>B2</sub> are important for G-protein activation by this receptor, although not absolutely required since the mutation of D688 into alanine, lysine or arginine does not prevent function.

*The GABA<sub>B2</sub> K572D/E mutants display a high agonist affinity*

In some cases, mutation of the arginine residue of the D/ERY motif of class A GPCRs leads to constitutively active receptors, as observed with the α1B adrenergic receptor receptors (43). Alternatively, such a mutation can result in a non-functional receptor that shares with constitutively active receptors high agonist affinity, such as for the Histamine H2 receptor (44). None of the mutations of K572 or R575 of the GABA<sub>B2</sub> lead to constitutive activity. We

therefore examined whether the mutation of these residues affects agonist affinity of the GABA<sub>B</sub> heterodimer. Binding experiments performed using the high affinity GABA<sub>B</sub> receptor antagonist [<sup>3</sup>H]-CGP54626 revealed that all mutants of K572 and R575 bind the corresponding non-radiolabeled antagonist CGP54626 with the same K<sub>i</sub> as on the wild type receptor (K<sub>i</sub> = 1.22±0.22 nM, 1.58±0.31 nM, 1.40±0.24 nM, and 1.57±0.23 nM for K572D, K572E, R575D, and wild-type receptors, respectively). Analysis of the affinity (K<sub>i</sub>) of the agonist GABA revealed that the K572D and K572E displayed a higher agonist affinity than the wild-type receptor or the K572A mutant (K<sub>i</sub> = 2.3±0.3 μM, 2.1±0.3 μM, 6.7±0.4 μM and 5.8±0.3 μM, respectively) (Fig.8A). In contrast, the R575D mutant displayed the same affinity for GABA as the wild-type receptor (K<sub>i</sub> = 6.8±0.8 μM) (Fig.8A). The same analysis was also performed on the D688E mutant that displays a higher constitutive activity than the wild-type receptor. As shown in Fig.8B, this constitutively active mutant also displays a higher affinity for GABA (K<sub>i</sub> = 3.7±0.5 μM and 6.7±0.4 μM for the D688E mutant and the wild-type, respectively). As a control, the affinity of the antagonist CGP54626 was not altered by the mutation (1.28±0.37 nM and 1.57±0.23 nM, for D688E and wild-type, respectively). The increase in agonist affinity is thus consistent with the conformation of the K572D/E mutated GABA<sub>B2</sub> HD resembling that of the active state.

## DISCUSSION

In the present study we identified two basic residues located in the cytoplasmic end of TM3, and one acidic residue located in the cytoplasmic end of TM6 highly conserved among class C GPCRs. We show that these residues (K572, R575 and D688 in GABA<sub>B2</sub>) play an important role in GABA<sub>B</sub> receptor activation.

The most conserved residue of class A GPCRs is the arginine of the D/ERY motif at the cytoplasmic side of TM3. Indeed, among the 3% mammalian rhodopsin-like GPCRs that lack this residue, none have been shown to activate G-proteins (45). Moreover, for the receptors lacking this basic residue, introduction of an arginine enables them to activate G-proteins, as shown for example for the C5A binding protein C5L2 (46) or the olfactory receptor 912-93 (47). In the inactive state of rhodopsin, this arginine residue makes an ionic interaction with the preceding glutamate of the ERY motif, and makes hydrogen bonds with E247 of TM6 (conserved in many GPCRs) (4,25),

and possibly T251 as shown in some models of rhodopsin (4). Disrupting this interaction network has been shown to either prevent G protein activation, or to stabilize the receptor in an active state. Indeed, protonation of the acidic residue of the ERY motif allows the arginine side chain to move and to make new contacts, and this could be a molecular step in the process leading to rhodopsin activation ((48) and reference therein). Moreover, neutralization of this acidic residue in many GPCRs results in their constitutive activation reinforcing the idea of its role in stabilizing the inactive state of the receptor (44,49-52). In contrast, mutation of the arginine residue leads to various phenotypes, either a loss (53-58), or a gain of function (43,59-61). In many cases, arginine mutations leading to loss of function are associated with a receptor conformation resembling that of the active state, as observed with the α1b adrenergic, the M1 muscarinic and the H2 histamine receptors (43,55,62,63). This may be the consequence of constitutive desensitization of the receptor as reported for a mutant of the V2 vasopressin receptor (64). Finally, the possible ionic interaction between this arginine and a conserved acidic residue of TM6 has been shown to maintain the β2 adrenergic, the α1b and the LH/hCG receptors in their inactive state (52,65-67). (52,65-67). The structure of an active state of rhodopsin has been solved recently and revealed only small conformational changes in the protein (68). However, it cannot be excluded that such limited conformational changes results from constraints from the crystal lattice, or from the absence of transducin. Using 3D modeling of rhodopsin-transducin complex, it has also been proposed that the arginine of the ERY motif directly contacts the G-protein (69), therefore playing a direct role in G-protein activation. Accordingly, two roles, not necessarily exclusive, have been proposed for the arginine of the D/ERY motif of class A GPCRs: 1) a stabilization of the inactive state through an ionic network involving TM6 residues, or 2) a direct role in G-protein interaction and activation.

Although the D/ERY motif is not found in class C GPCRs, two basic residues are highly conserved at an equivalent position (at the cytoplasmic end of TM3) in these receptors. Moreover, like arginine of the D/ERY motif, 3D models suggest that their side chains are directed towards or facing TM6 where a conserved acidic residue is located. Mutation of the more C-terminal basic residue R575 in GABA<sub>B2</sub> resulted in a loss of function and suppression of the constitutive activity of the receptor, even though

the cell surface expression of the mutants was normal. The loss of function of the R575D/E mutants cannot be restored by replacing D688 of TM6 by a basic residue. Finally, agonist affinity is not affected by such mutation, indicating that arginine mutation does not convert the receptor into an active-like conformation uncoupled to G-proteins. Accordingly, this arginine appears necessary for G-protein activation, but the exact reason for this is not clear. As in our GABA<sub>B2</sub> model, the arginine residue R575 is oriented toward the G protein, it is possible that this arginine is required for the proper interaction with the G-protein as proposed for R135 of rhodopsin (69). In agreement with this possibility, arginine 575 points toward the cytoplasm, in a cavity between the intracellular loops 2 and 3 (Fig.2B) known to contact the G $\alpha$  protein in class C GPCRs (70-72). However, this arginine is not conserved in some class C GPCRs such as the taste T1Rs and mGlu3, despite their known capacity to activate G-proteins.

The other conserved basic residue in TM3 of class C GPCRs is a lysine that is located one turn of a helix above the arginine. Replacement of the lysine by an acidic residue resulted in a total loss of function that could be partly restored by mutating D688 of TM6 into arginine or lysine. This likely results from an ionic interaction between the two mutated residues. This is surprising when considering that the K572A and the four mutants of D688 are functional indicating that an ionic interaction between these two positions is not absolutely required for function. However, this does not exclude an ionic interaction between K572 and D688, since other interactions between TM3 and TM6 may still maintain the correct relative positioning of these helices in the absence of D688. Of interest, equivalent mutations of the corresponding acidic residue in TM6 in the calcium-sensing receptor lead to a non functional receptor (73,74). If K572 and D688 are facing each other, mutation of K572 into an acidic residue may result in a repulsion of TM3 and TM6, resulting in a change in conformation of the GABA<sub>B2</sub> HD. Consistent with this proposal, K572D/E mutants display a higher affinity for GABA. Of interest, increasing the length of the acidic side chain of TM6 by replacing D688 by glutamate also increases agonist affinity, consistent with the high agonist affinity state resulting from a movement of TM6 relative to TM3. It is surprising that the mutation of D688 into a basic residue did not have the same effect despite the presence of positive charges in both TM3 and TM6. However, the length of the

side chains of lysine and arginine is such that the repulsion of the charges may not necessarily affect the relative positions of the helices.

Whereas the higher agonist affinity state of the D688E and K572D/E mutants may possibly correspond to an active state, only the D688E mutant displays a higher constitutive activity, the K572D/E mutants being inactive. The loss of function of K572D/E does not result from a constitutive desensitization of the GABA<sub>B</sub> receptor, as reported for a mutant of the V2 vasopressin receptor (64), for several reasons. First, this mutant is still expressed normally at the cell surface, indicating that internalization cannot be responsible for the loss of function. Indeed, the GABA<sub>B</sub> receptor internalizes neither in HEK293 cells nor in neurons even after long term activation by agonist (75,76). Second, desensitization of the GABA<sub>B</sub> receptor has been observed only in the presence of GRK4 that is not expressed in HEK 293 cells (75). Moreover, the basal activity of a fully constitutively active GABA<sub>B</sub> receptor can easily be measured in these cells with our assay (77). Accordingly, the K572D/E mutants may be in a specific inactive conformation that is however associated with higher agonist affinity. Alternatively, this mutant may be in an active conformation, but unable to activate G-proteins. As shown above, R575 is crucial for G-protein activation by this receptor. This arginine may well interact with the acidic residue at position 572, one turn of  $\alpha$  helix above, in the K572E mutant (Fig. 2 and 9), therefore preventing G-protein activation. In agreement with this proposal, the double mutation inverting the charges at the bottom of TM3 and TM6 (K572D/E and D688K/R) restores receptor function. In this mutant, the reintroduction of the ionic interaction between these TMs likely allows R575 to play its own role in G-protein activation (Fig.9).

Our data further illustrate the critical role of the GABA<sub>B2</sub> HD in G-protein activation by the heterotrimeric GABA<sub>B</sub> receptor. Indeed, consistent with previous studies (36,38), single point mutations in the GABA<sub>B2</sub> HD are sufficient to suppress G-protein activation by the heterodimer whereas the equivalent mutations in the GABA<sub>B1</sub> HD have no effect. It is however interesting to note that both the lysine and the acidic residues of TM3 and 6 respectively, are conserved in GABA<sub>B1</sub> (Fig. 1A). In contrast, the arginine residue, although conserved in the *C. elegans* and *Drosophila* GABA<sub>B1</sub> subunit, is replaced by a tryptophane in vertebrates (Fig. 1A). However, replacement of this tryptophane by an

arginine was not sufficient to allow this GABA<sub>B</sub> receptor subunit to activate G-proteins in the absence of GABA<sub>B2</sub>, or in the presence of a non-functional GABA<sub>B2</sub> subunit (unpublished data). This is in agreement with the absence of function of the drosophila GABA<sub>B1</sub> that still possesses the arginine (78), and further indicates that other specific constraints prevent GABA<sub>B1</sub> subunit from activating G-proteins.

Taken together, these data highlight the importance of charged residues at the cytoplasmic ends of TM3 and TM6 of class C GPCRs in a dynamic network of interactions

controlling activation of the receptor, as already established for many class A GPCRs. Indeed, each of the two conserved basic residues of class C TM3 plays one of the proposed roles of the arginine of the D/ERY motif of class A GPCRs: the lysine residue being involved in an ionic interaction with TM6, while the arginine plays a direct role in G-protein activation. These data revealed that despite their modular structure and their constitutive dimeric organization, the HDs of class C GPCRs share more functional similarities with those of class A GPCRs than originally thought.

## REFERENCES

1. Bockaert, J., Claeysen, S., Becamel, C., Pinloche, S., and Dumuis, A. (2002) *Int Rev Cytol* **212**, 63-132
2. Karnik, S. S., Gogonea, C., Patil, S., Saad, Y., and Takezako, T. (2003) *Trends Endocrinol Metab* **14**, 431-437
3. Gether, U. (2000) *Endocr Rev* **21**, 90-113
4. Palczewski, K., Kumasaka, T., Hori, T., Behnke, C. A., Motoshima, H., Fox, B. A., Le Trong, I., Teller, D. C., Okada, T., Stenkamp, R. E., Yamamoto, M., and Miyano, M. (2000) *Science* **289**, 739-745
5. Fredriksson, R., Lagerstrom, M. C., Lundin, L. G., and Schioth, H. B. (2003) *Mol Pharmacol* **63**, 1256-1272.
6. Foord, S. M., Bonner, T. I., Neubig, R. R., Rosser, E. M., Pin, J. P., Davenport, A. P., Spedding, M., and Harmar, A. J. (2005) *Pharmacol Rev* **57**, 279-288
7. Lu, Z. L., Saldanha, J. W., and Hulme, E. C. (2002) *Trends Pharmacol Sci* **23**, 140-146
8. Flanagan, C. A. (2005) *Mol Pharmacol* **68**, 1-3
9. Perez, D. M., and Karnik, S. S. (2005) *Pharmacol Rev* **57**, 147-161
10. Pin, J.-P., Galvez, T., and Prezeau, L. (2003) *Pharmacol Ther* **98**, 325-354
11. Pin, J. P., Kniazeff, J., Goudet, C., Bessis, A. S., Liu, J., Galvez, T., Acher, F., Rondard, P., and Prezeau, L. (2004) *Biol Cell* **96**, 335-342
12. Pin, J. P., Kniazeff, J., Liu, J., Binet, V., Goudet, C., Rondard, P., and Prezeau, L. (2005) *Febs J* **272**, 2947-2955
13. Tateyama, M., Abe, H., Nakata, H., Saito, O., and Kubo, Y. (2004) *Nat Struct Mol Biol* **11**, 637-642
14. Pagano, A., Ruegg, D., Litschig, S., Stoehr, N., Stierlin, C., Heinrich, M., Floersheim, P., Prezeau, L., Carroll, F., Pin, J. P., Cambria, A., Vranesic, I., Flor, P. J., Gasparini, F., and Kuhn, R. (2000) *J Biol Chem* **275**, 33750-33758
15. Goudet, C., Gaven, F., Kniazeff, J., Vol, C., Liu, J., Cohen-Gonsaud, M., Acher, F., Prezeau, L., and Pin, J. P. (2004) *Proc Natl Acad Sci U S A* **101**, 378-383
16. Goudet, C., Binet, V., Prezeau, L., and Pin, J.-P. (2004) *Drug Discovery Today: Therap. Strategies* **1**, 125-133
17. Binet, V., Brajon, C., Le Corre, L., Acher, F., Pin, J. P., and Prezeau, L. (2004) *J Biol Chem* **279**, 29085-29091
18. Ray, K., Tisdale, J., Dodd, R. H., Dauban, P., Ruat, M., and Northup, J. K. (2005) *J Biol Chem* **280**, 37013-37020

19. Pagano, A., Rovelli, G., Mosbacher, J., Lohmann, T., Duthey, B., Stauffer, D., Ristig, D., Schuler, V., Heid, J., Meigel, I., Lampert, C., Stein, T., Prézeau, L., Pin, J.-P., Froestl, W., Kuhn, R., Kaupmann, K., and Bettler, B. (2001) *J. Neurosci.* **21**, 1189–1202
20. Galvez, T., Duthey, B., Kniazeff, J., Blahos, J., Rovelli, G., Bettler, B., Prezeau, L., and Pin, J. P. (2001) *Embo J* **20**, 2152-2159.
21. Liu, J., Maurel, D., Etzol, S., Brabet, I., Pin, J.-P., and Rondard, P. (2004) *J. Biol. Chem.* **279**, 15824-15830
22. Higgins, D., Thompson, J., Gibson, T., Thompson, J. D., Higgins, D. G., and Gibson, T. J. (1994) *Nucleic Acids Res.*, 4673-4680
23. Douguet, D., and Labesse, G. (2001) *Bioinformatics* **17**, 752–753
24. Okada, T., Sugihara, M., Bondar, A. N., Elstner, M., Entel, P., and Buss, V. (2004) *J Mol Biol* **342**, 571-583
25. Li, J., Edwards, P. C., Burghammer, M., Villa, C., and Schertler, G. F. (2004) *J Mol Biol* **343**, 1409-1438
26. Catherinot, V., and Labesse, G. (2004) *Bioinformatics* **20**, 3694-3696
27. Canutescu, A., Shelenkov, A., and Dunbrack, R. J. (2003) *Protein Sci.* **12**, 2001-2014
28. Sali, A., and Blundell, T. L. (1993) *J. Mol. Biol.* **234**, 779–815
29. Jiang, P., Cui, M., Zhao, B., Liu, Z., Snyder, L. A., Benard, L. M., Osman, R., Margolskee, R. F., and Max, M. (2005) *J Biol Chem* **280**, 15238-15246
30. Miedlich, S. U., Gama, L., Seuwen, K., Wolf, R. M., and Breitwieser, G. E. (2004) *J Biol Chem* **279**, 7254-7263
31. Malherbe, P., Kratochwil, N., Knoflach, F., Zenner, M. T., Kew, J. N., Kratzeisen, C., Maerki, H. P., Adam, G., and Mutel, V. (2003) *J Biol Chem* **278**, 8340-8347
32. Malherbe, P., Kratochwil, N., Zenner, M. T., Piussi, J., Diener, C., Kratzeisen, C., Fischer, C., and Porter, R. H. (2003) *Mol Pharmacol* **64**, 823-832
33. Petrel, C., Kessler, A., Maslah, F., Dauban, P., Dodd, R. H., Rognan, D., and Ruat, M. (2003) *J Biol Chem* **278**, 49487-49494
34. Kniazeff, J., Galvez, T., Labesse, G., and Pin, J. P. (2002) *J Neurosci* **22**, 7352-7361.
35. Galvez, T., Parmentier, M. L., Joly, C., Malitschek, B., Kaupmann, K., Kuhn, R., Bittiger, H., Froestl, W., Bettler, B., and Pin, J. P. (1999) *J Biol Chem* **274**, 13362-13369
36. Duthey, B., Caudron, S., Perroy, J., Bettler, B., Fagni, L., Pin, J. P., and Prezeau, L. (2002) *J Biol Chem* **277**, 3236-3241.
37. Margeta-Mitrovic, M., Jan, Y. N., and Jan, L. Y. (2001) *Proc Natl Acad Sci U S A* **98**, 14649-14654.
38. Robbins, M. J., Calver, A. R., Filippov, A. K., Hirst, W. D., Russell, R. B., Wood, M. D., Nasir, S., Couve, A., Brown, D. A., Moss, S. J., and Pangalos, M. N. (2001) *J Neurosci* **21**, 8043-8052.
39. Brock, C., Boudier, L., Maurel, D., Blahos, J., and Pin, J. P. (2005) *Mol Biol Cell* **16**, 5572-5578
40. Couve, A., Filippov, A. K., Connolly, C. N., Bettler, B., Brown, D. A., and Moss, S. J. (1998) *J Biol Chem* **273**, 26361-26367.
41. Margeta-Mitrovic, M., Jan, Y. N., and Jan, L. Y. (2000) *Neuron* **27**, 97-106
42. Gomeza, J., Mary, S., Brabet, I., Parmentier, M.-L., Restituito, S., Bockaert, J., and Pin, J.-P. (1996) *Mol. Pharmacol.* **50**, 923-930
43. Scheer, A., Costa, T., Fanelli, F., De Benedetti, P. G., Mhaouty-Kodja, S., Abuin, L., Nenniger-Tosato, M., and Cotecchia, S. (2000) *Mol Pharmacol* **57**, 219-231.
44. Alewijnse, A. E., Timmerman, H., Jacobs, E. H., Smit, M. J., Roovers, E., Cotecchia, S., and Leurs, R. (2000) *Mol Pharmacol* **57**, 890-898

45. Rosenkilde, M. M., Kledal, T. N., and Schwartz, T. W. (2005) *Mol Pharmacol* **68**, 11-19
46. Okinaga, S., Slattery, D., Humbles, A., Zsengeller, Z., Morteau, O., Kinrade, M. B., Brodbeck, R. M., Krause, J. E., Choe, H. R., Gerard, N. P., and Gerard, C. (2003) *Biochemistry* **42**, 9406-9415
47. Gaillard, I., Rouquier, S., Chavanieu, A., Mollard, P., and Giorgi, D. (2004) *Hum Mol Genet* **13**, 771-780
48. Menon, S., Han, M., and Sakmar, T. (2001) *Pharmacol Review* **81**, 1659-1688
49. Capra, V., Veltri, A., Foglia, C., Crimaldi, L., Habib, A., Parenti, M., and Rovati, G. E. (2004) *Mol Pharmacol* **66**, 880-889
50. Scheer, A., and Cotecchia, S. (1997) *J Recept Signal Transduct Res* **17**, 57-73.
51. Rasmussen, S. G., Jensen, A. D., Liapakis, G., Ghanouni, P., Javitch, J. A., and Gether, U. (1999) *Mol Pharmacol* **56**, 175-184
52. Ballesteros, J. A., Shi, L., and Javitch, J. A. (2001) *Mol Pharmacol* **60**, 1-19.
53. Rosenthal, W., Antaramian, A., Gilbert, S., and Birnbaumer, M. (1993) *J Biol Chem* **268**, 13030-13033
54. Acharya, S., and Karnik, S. S. (1996) *J Biol Chem* **271**, 25406-25411
55. Scheer, A., Fanelli, F., Costa, T., De Benedetti, P. G., and Cotecchia, S. (1996) *Embo J* **15**, 3566-3578.
56. Lu, Z. L., Curtis, C. A., Jones, P. G., Pavia, J., and Hulme, E. C. (1997) *Mol Pharmacol* **51**, 234-241
57. Gruijthuisen, Y. K., Beuken, E. V., Smit, M. J., Leurs, R., Bruggeman, C. A., and Vink, C. (2004) *J Gen Virol* **85**, 897-909
58. Wess, J. (1998) *Pharmacol Ther* **80**, 231-264
59. Seibold, A., Dagarag, M., and Birnbaumer, M. (1998) *Receptors Channels* **5**, 375-385
60. Fanelli, F., Menziani, C., Scheer, A., Cotecchia, S., and De Benedetti, P. G. (1999) *Proteins* **37**, 145-156
61. Chen, A., Gao, Z. G., Barak, D., Liang, B. T., and Jacobson, K. A. (2001) *Biochem Biophys Res Commun* **284**, 596-601
62. Wilbanks, A. M., Laporte, S. A., Bohn, L. M., Barak, L. S., and Caron, M. G. (2002) *Biochemistry* **41**, 11981-11989
63. Jones, P. G., Curtis, C. A., and Hulme, E. C. (1995) *Eur J Pharmacol* **288**, 251-257
64. Barak, L. S., Oakley, R. H., Laporte, S. A., and Caron, M. G. (2001) *Proc Natl Acad Sci U S A* **98**, 93-98
65. Greasley, P. J., Fanelli, F., Rossier, O., Abuin, L., and Cotecchia, S. (2002) *Mol Pharmacol* **61**, 1025-1032
66. Shenker, A., Laue, L., Kosug, S., Merendino, J. J., Minegishi, T., and Cutler, J. B. (1993) *Nature* **365**, 652-654
67. Yano, K., Saji, M., Hidaka, A., Moriya, N., Okuno, A., Kohn, L. D., and Cutler, G. B., Jr. (1995) *J Clin Endocrinol Metab* **80**, 1162-1168
68. Salom, D., Lodowski, D. T., Stenkamp, R. E., Trong, I. L., Golczak, M., Jastrzebska, B., Harris, T., Ballesteros, J. A., and Palczewski, K. (2006) *Proc Natl Acad Sci U S A* **103**, 16123-16128
69. Filipek, S., Krzysko, K. A., Fotiadis, D., Liang, Y., Saperstein, D. A., Engel, A., and Palczewski, K. (2004) *Photochem Photobiol Sci* **3**, 628-638
70. Pin, J.-P., Joly, C., Heinemann, S. F., and Bockaert, J. (1994) *EMBO J.* **13-2**, 342-348
71. Havlickova, M., Blahos, J., Brabet, I., Liu, J., Hruskova, B., Prezeau, L., and Pin, J. P. (2003) *J Biol Chem* **278**, 35063-35070
72. Gomeza, J., Joly, C., Kuhn, R., Knopfel, T., Bockaert, J., and Pin, J. P. (1996) *J Biol Chem* **271**, 2199-2205
73. Francesconi, A., and Duvoisin, R. M. (1998) *J Biol Chem* **273**, 5615-5624.

74. Chang, W., Chen, T. H., Pratt, S., and Shoback, D. (2000) *J Biol Chem* **275**, 19955-19963.
75. Perroy, J., Adam, L., Qanbar, R., Chenier, S., and Bouvier, M. (2003) *Embo J* **22**, 3816-3824
76. Couve, A., Restituito, S., Brandon, J. M., Charles, K. J., Bawagan, H., Freeman, K. B., Pangalos, M. N., Calver, A. R., and Moss, S. J. (2004) *J Biol Chem* **279**, 13934-13943
77. Kniazeff, J., Saintot, P.-P., Goudet, C., Liu, J., Charnet, A., Guillon, G., and Pin, J.-P. (2004) *J. Neuroscience* **24**, 370-377
78. Mezler, M., Muller, T., and Raming, K. (2001) *Eur J Neurosci* **13**, 477-486.

#### ACKNOWLEDGEMENTS

This work was supported by grants from the Centre National de la Recherche Scientifique (CNRS), Action Concertée Incitative ACI-BCMS (328, contract number 45 491 to JPP), the French Ministry of Research (ANR-05-NEUR-035), the European Community EEC STREP program GPCR from the 6<sup>th</sup>PCRD (LSHB-CT-2003-503337 to JPP), and contracts with Addex Pharmaceuticals.

We would like to thank T. Durroux for helpful discussion and reading.

#### FIGURE LEGENDS

Fig. 1. Alignment of the sequences of class C GPCRs. Three conserved residues at the cytoplasmic face of TM3 and TM6 were chosen, as their positions are close to the positions of the D/ERY and D/E motifs in TM3 and TM6 rhodopsin, respectively. The notation of most of the sequences are after the SwissProt data bank notation, with the following accession numbers: MGR5\_RAT P31424, MGR1\_RAT P23385, MGR1\_CAEL Q09630, MGR\_DROME P91685, MGR7\_RAT P35400, MGR6\_RAT P35349, MGR8\_RAT P70579, CASR\_MOUSE Q9QY96, TS1R1\_RAT Q9Z0R8, GABR1\_RAT Q9Z0U4, GABR2\_RAT O88871, and OPSD\_BOVIN P02699. AAK13420 and AAK13421 sequence, that are GABA<sub>B</sub> subunits homologues from drosophila, are notated after their gene bank names.

Fig. 2. Molecular modeling of GABA<sub>B2</sub>. A. The side chains of the residues conserved in the GABA<sub>B</sub> subunits from different species (rat, human, coenorhabditis elegans, and drosophila melanogaster) are showed in black. The representation of the model is viewed from the extracellular side, with the helical TMs showed in ribbon representation. B. The residues K572 and R575 in TM3, and D688 in TM6, are shown in wireframe and in color according to the atom types. The two cysteins conserved in the class C receptors and corresponding to the conserved cysteins in class A receptors involved in a disulfide bridge at the extracellular face are also showed. The representation of the model is viewed from the side and shows the helical TMs in ribbon representation. Loops are shown in white/grey, while TMs are colored as following: TM1 in red, TM2 in brown, TM3 in orange, TM4 in green, TM5 in dark green, TM6 in cyan, and TM7 in dark blue. The figures have been made using the program ViTO.

Fig. 3. Expression at the cell surface and functional assay of the receptors containing a mutated GABA<sub>B2</sub> subunit. A. The cell surface expression of the receptors was analyzed using an ELISA method on intact cells and by detecting the presence of the GABA<sub>B1</sub> subunit tagged at its extracellular end by a HA epitope. As GABA<sub>B1</sub> reaches the cell surface only when associated with GABA<sub>B2</sub>, the detection of the GABA<sub>B1</sub> at the cell surface indicates that GABA<sub>B2</sub> was folded and able to interact correctly with GABA<sub>B1</sub> and to take it to the cell surface. The data are the means ± sem of at least three independent experiments performed in triplicates. B. In functional assays, the ligand-induced activity of the mutated receptors was assayed by quantifying the accumulating InP second messenger molecules formed upon activation of the receptors by GABA 1mM. To get coupled to the InP pathway, the GABA<sub>B</sub> receptor is expressed with the Gqi9 chimeric G protein (see Material and Methods). The data are the means ± sem of at least four independent experiments performed in triplicates.

Fig. 4. Expression at the cell surface and functional assay of the receptors containing a mutated GABA<sub>B1</sub> subunit. A. The cell surface expression of the receptors was analyzed using an ELISA method on intact cells as described in figure 3. The data are the means ± sem of at least three independent experiments performed in triplicates. B. The ligand-induced activity of the mutated receptors was measured as described in figure 3. The data are the means ± sem of at least for independent experiments performed in triplicates.

Fig. 5. Expression at the cell surface and functional assay of the receptors containing the GABA<sub>B2</sub> subunit bearing the double mutation of K572 and D688. A. The cell surface expression of the receptors was analyzed using an ELISA method on intact cells as described in figure 3. The data are the means ± sem of at least three independent experiments performed in triplicates. B. Functional responses of mutated receptors. The ligand-induced activity of the mutated receptors was measured as described in figure 3. The data are the means ± sem of at least three independent experiments performed in triplicates.

Fig. 6. Expression at the cell surface and functional assay of the receptors containing the GABA<sub>B2</sub> subunit bearing the double mutation of R575 and D688. A. The cell surface expression of the receptors was analyzed using an ELISA method on intact cells as described in figure 3. The data are the means ± sem of at least three independent experiments performed in triplicates. B. Functional responses of mutated receptors. The ligand-induced activity of the mutated receptors was measured as described in figure 3. The data are the means ± sem of at least three independent experiments performed in triplicates.

Fig. 7. A. Dose-response curves of the receptor in a functional InP assay. The mutated receptor activity was measured in the presence of increasing concentrations of GABA. The indicated GABA<sub>B2</sub> subunits were expressed together with the wild-type GABA<sub>B1</sub> subunit and the Gqi9 chimeric G protein. See Material and Methods for details. This experiment is representative of three independent experiments performed in triplicates.

Fig. 8. Displacement curves of the radioligand [<sup>3</sup>H]CGP54626 by increasing concentrations of GABA, on wild-type and mutated GABA<sub>B</sub> receptor. The indicated GABA<sub>B2</sub> subunits were expressed together with the wild-type GABA<sub>B1</sub> subunit. See Material and Methods for details. A. Displacement curves on the wild-type GABA<sub>B</sub> receptor and on receptors bearing the mutations K572D, E or A and R575D. This experiments is representative of three independent experiments performed in triplicates. B. Displacement curves on the wild-type GABA<sub>B</sub> receptor and on receptors bearing the mutation D688E. This experiment is representative of three independent experiments performed in triplicates.

Fig. 9. Putative functional role of the residues K572, R575, and D688 at the interface of the TM3 and TM6 of GABA<sub>B2</sub>. A. Three-dimensional model of the mutated GABA<sub>B2</sub>. For clarity, only the region of the mutated residues (K572, R575, and D688) is shown. The structure rendering and the color code used are as in Fig 2. B. Schematic representation of the putative effect of the mutation K572D and of the reversing effect of the double mutation K572D-D688K in GABA<sub>B2</sub> deduced from the experimental data and the structural analysis.

A

TM3

TM6

	* *	*
MGR5_RAT	AMSYSALVT <b>KTNR</b> IARILAGS <del>KKK</del>	ANFN <b>EA</b> KYIAFTMYTT
MGR1_RAT	AMCYSALVT <b>KTNR</b> IARILAGS <del>KKK</del>	ANFN <b>EA</b> KYIAFTMYTT
MGR1_CAEL	SCLYSAMFV <b>KTNR</b> IFRIFS--TRS	ENFN <b>ET</b> KFIGFSMYTT
MGR_DROME	SIIYSALL <b>KTNR</b> ISRIFHSASKS	ENFN <b>ES</b> KFIGFTMYTT
MGR7_RAT	CISYAALL <b>KTNR</b> IYRIFEQGKKS	ENFN <b>EA</b> KPIGFTMYTT
MGR6_RAT	TLSYSALL <b>KTNR</b> IYRIFEQKRS	ETFN <b>EA</b> KPIGFTMYTT
MGR8_RAT	CFSYAALL <b>KTNR</b> IHRIFEQGKKS	ETFN <b>EA</b> KPIGFTMYTT
CASR_MOUSE	VLCISCILV <b>KTNR</b> VLLVFEAKIPT	ENFN <b>EA</b> KFITFSMLIF
TS1R1_RAT	AIFLSCLT <b>IR</b> SFQLV <del>I</del> IFKFSTKV	ENYN <b>EA</b> KCVTFSLLLN
GABR1B_RAT	SLGYGSMFT <b>KI</b> WWHTVFTKKEEK	EKIND <b>H</b> RAVGMAIYNV
AAK13420	TLAYGAMF <b>SKV</b> RVHRFTTKAKTD	KOIND <b>S</b> RYVGMSIYNV
GABR2_RAT	TTAFGAMF <b>AKT</b> WRVHAIFKNVKMK	PALND <b>S</b> KYIGMSVYNV
AAK13421	SLSFGAMF <b>SKT</b> WRVHSIFDLKLN	PALND <b>S</b> KHIGFSVYNV
	***	*
OPSD_BOVIN	EIALWLVVLA <b>IERY</b> VVVCKPMSN	A <b>E</b> KEVTRMVIIMVIAF

Fig.1

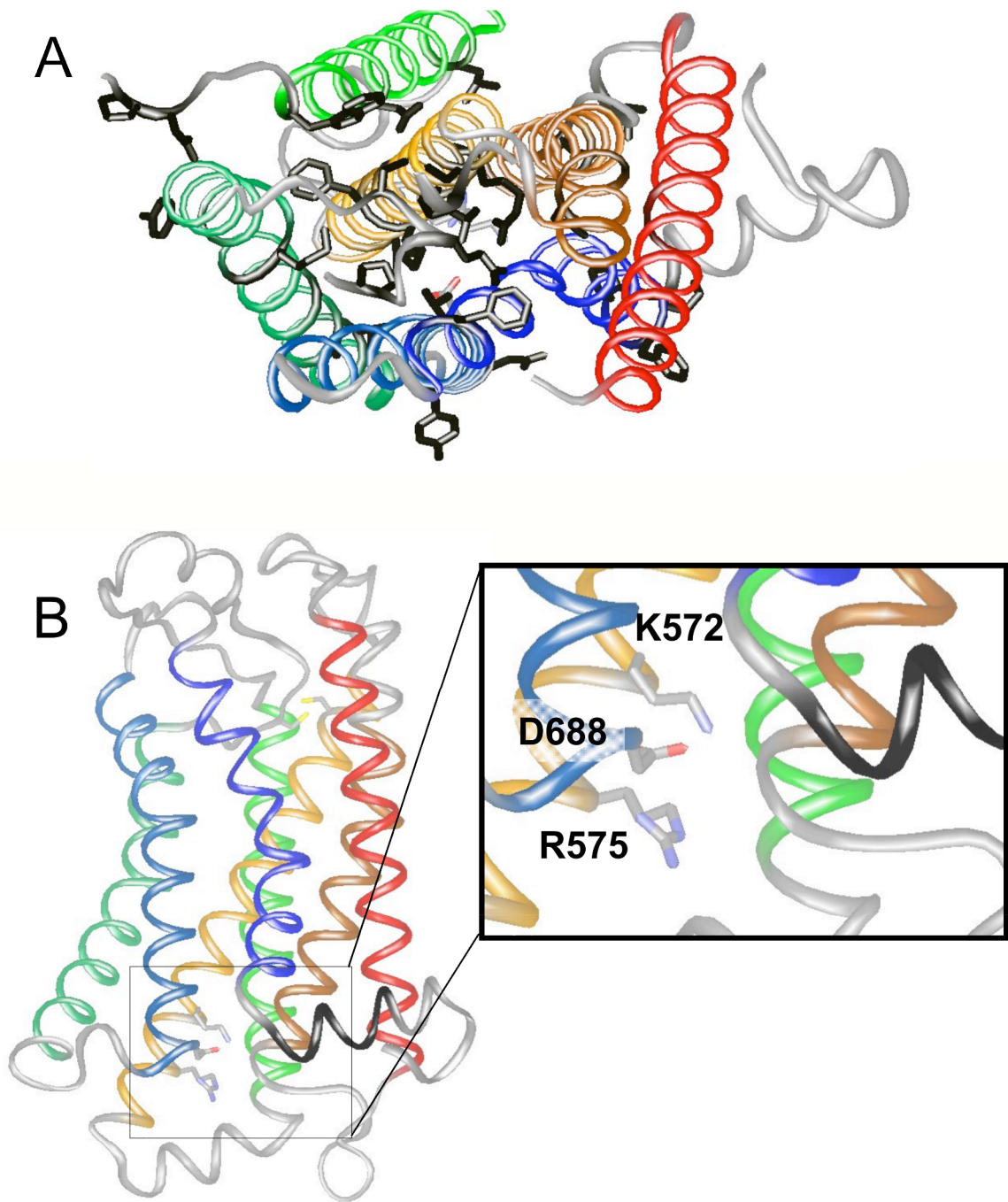


Fig.2

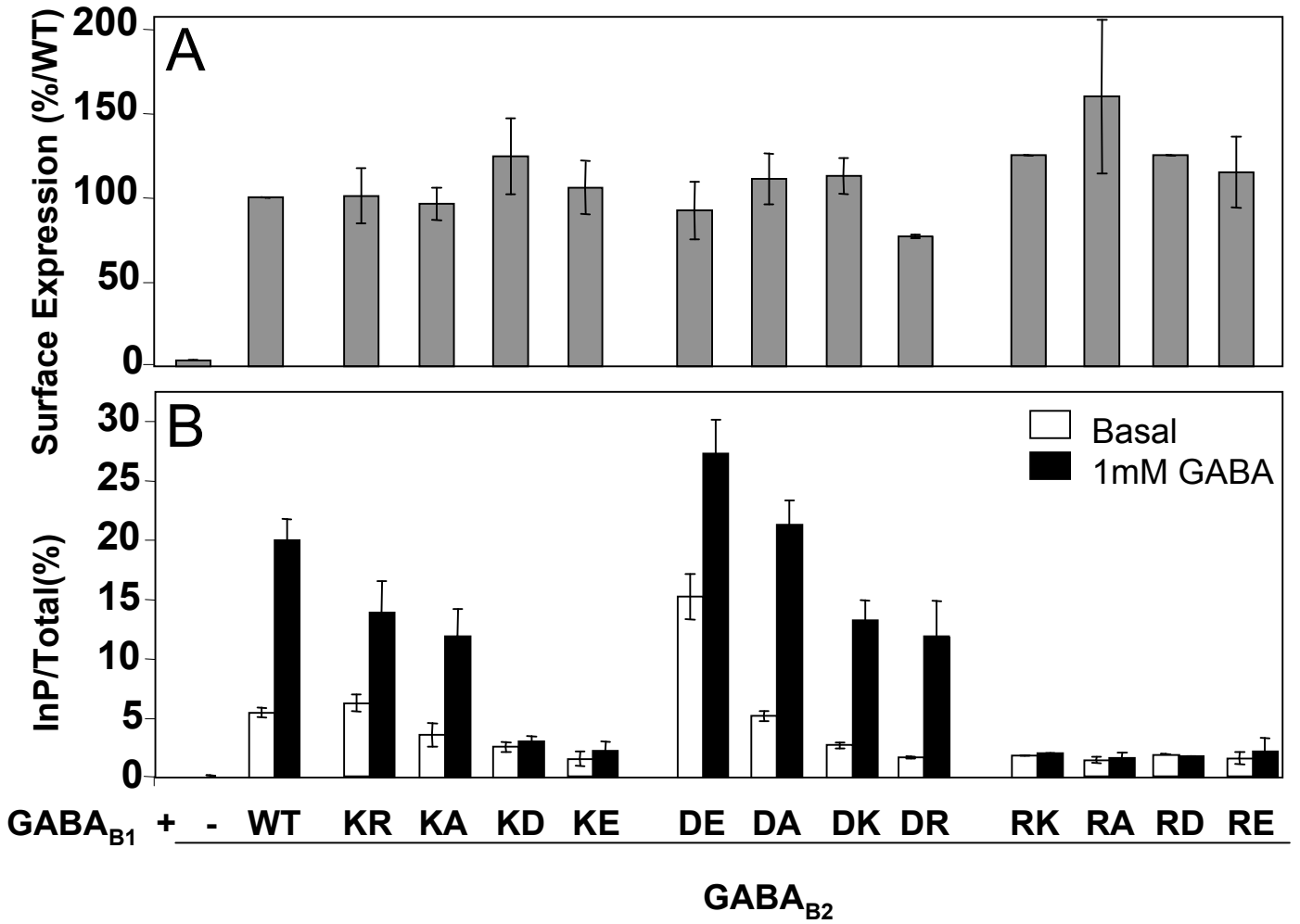


Fig.3

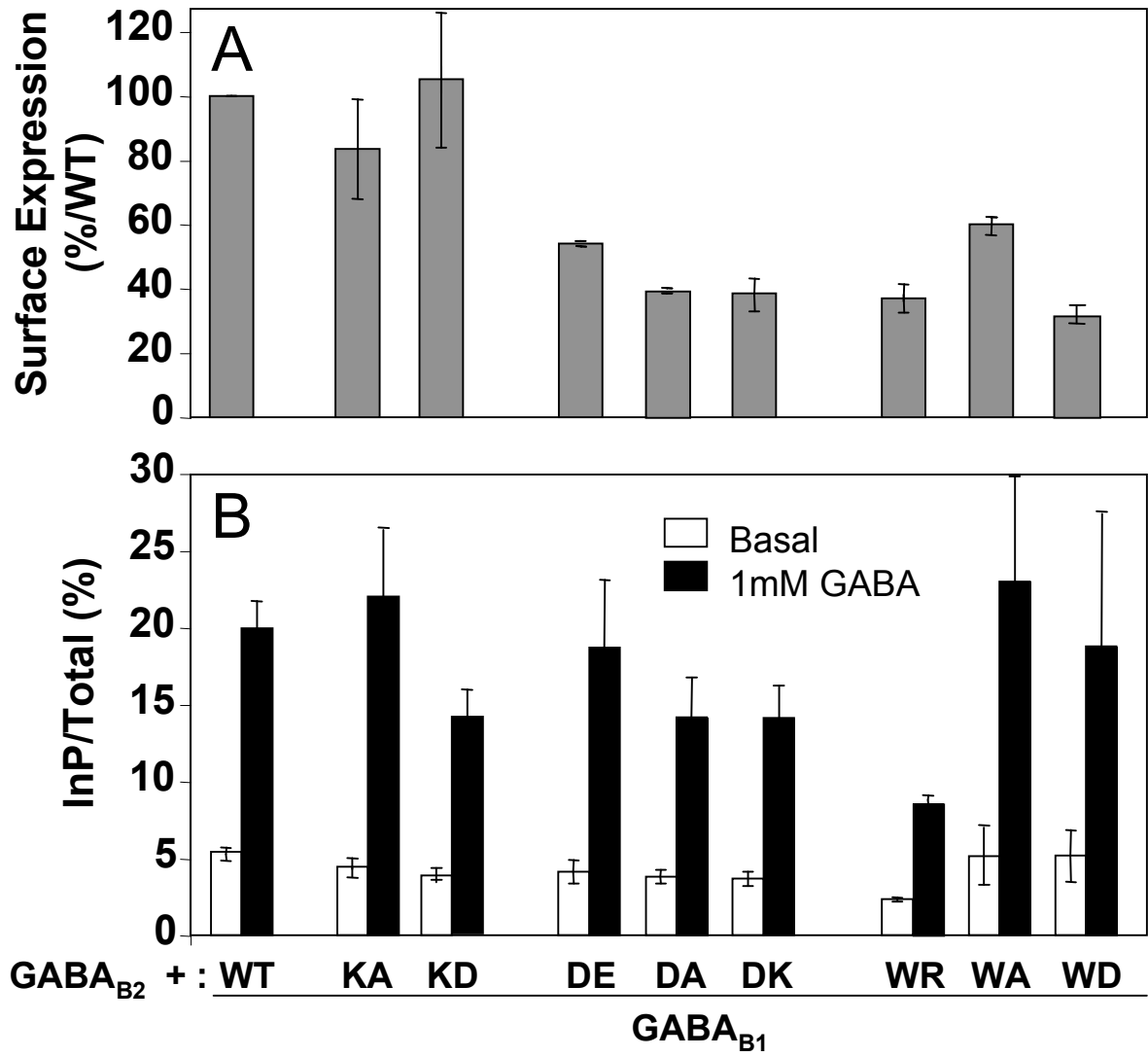


Fig.4

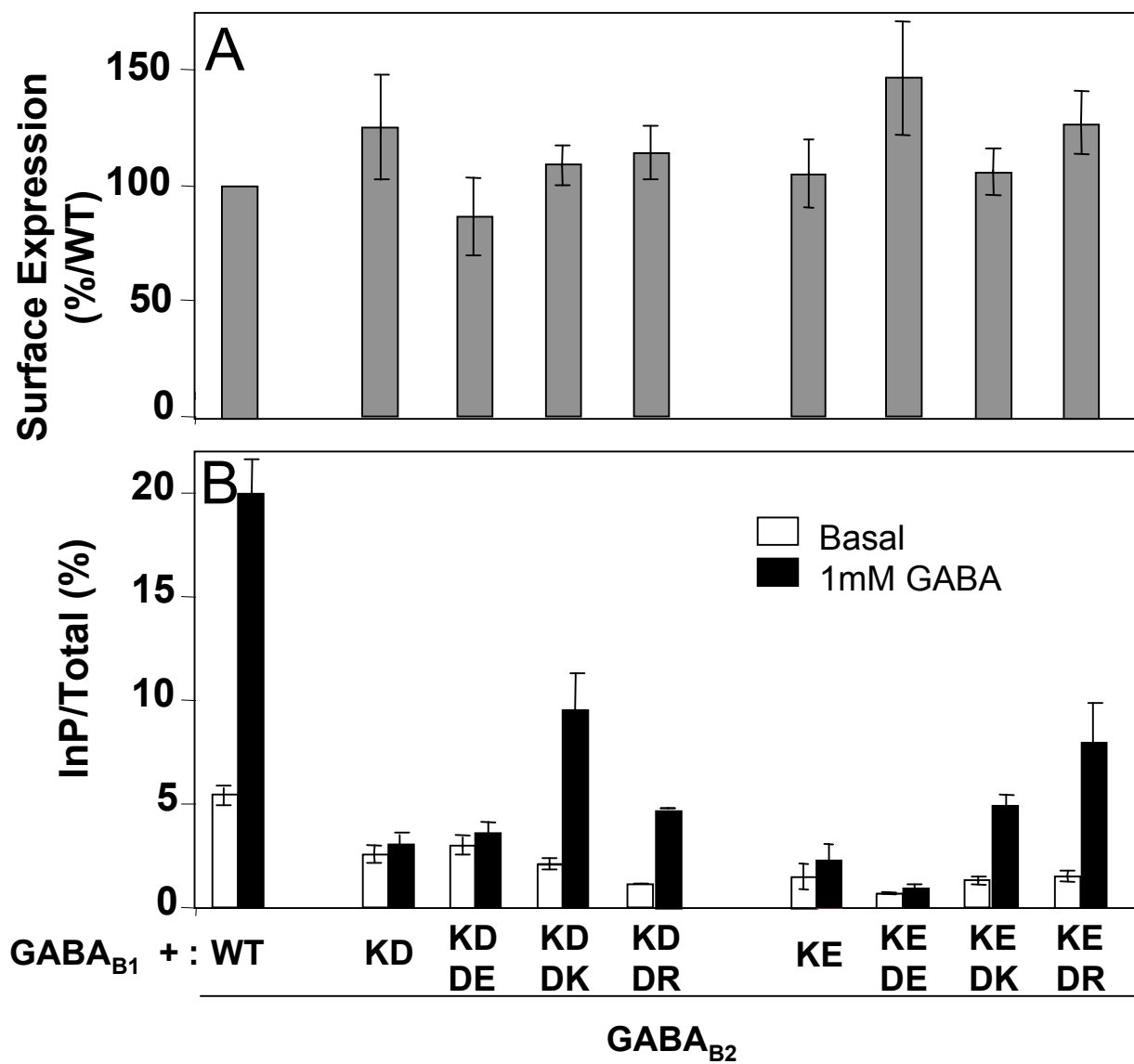


Fig.5

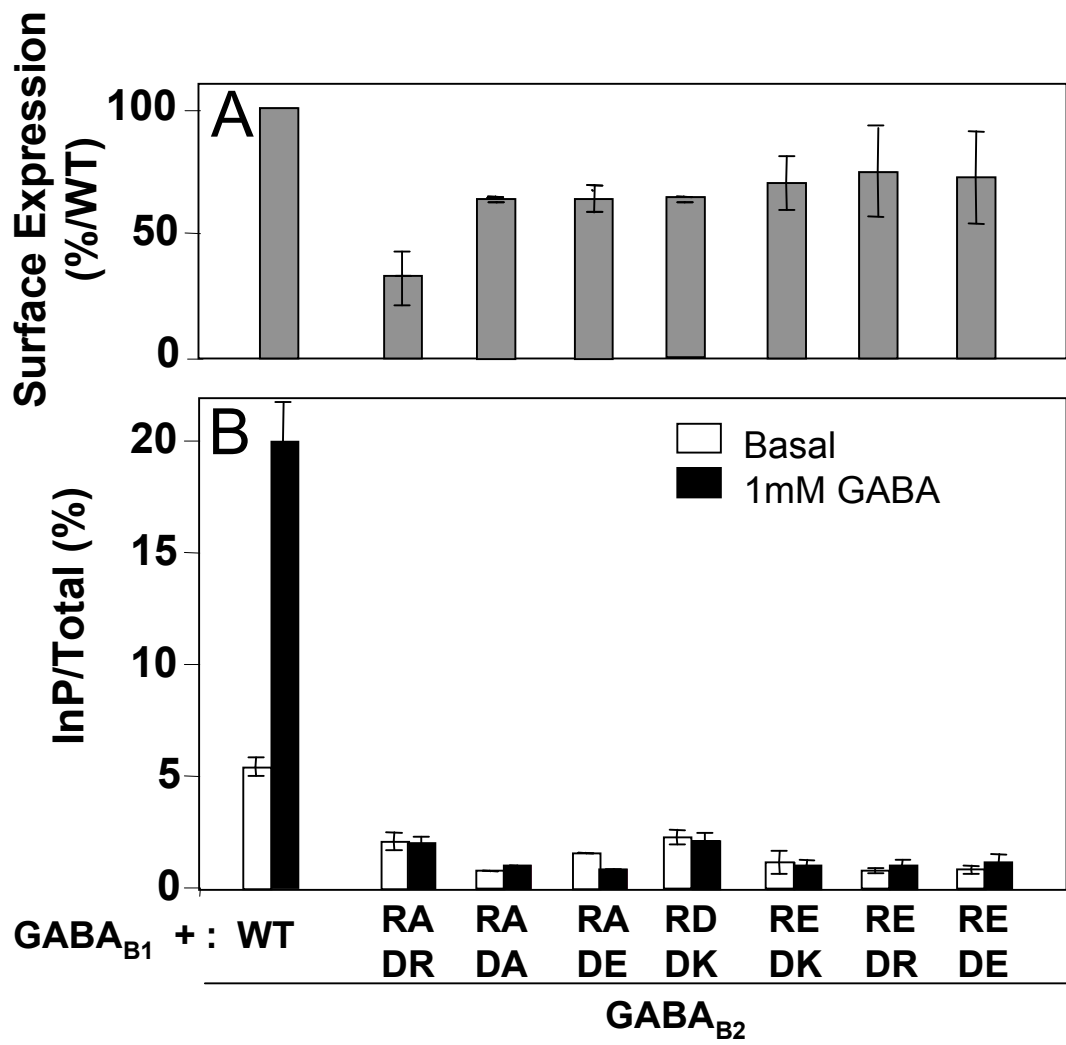


Fig.6

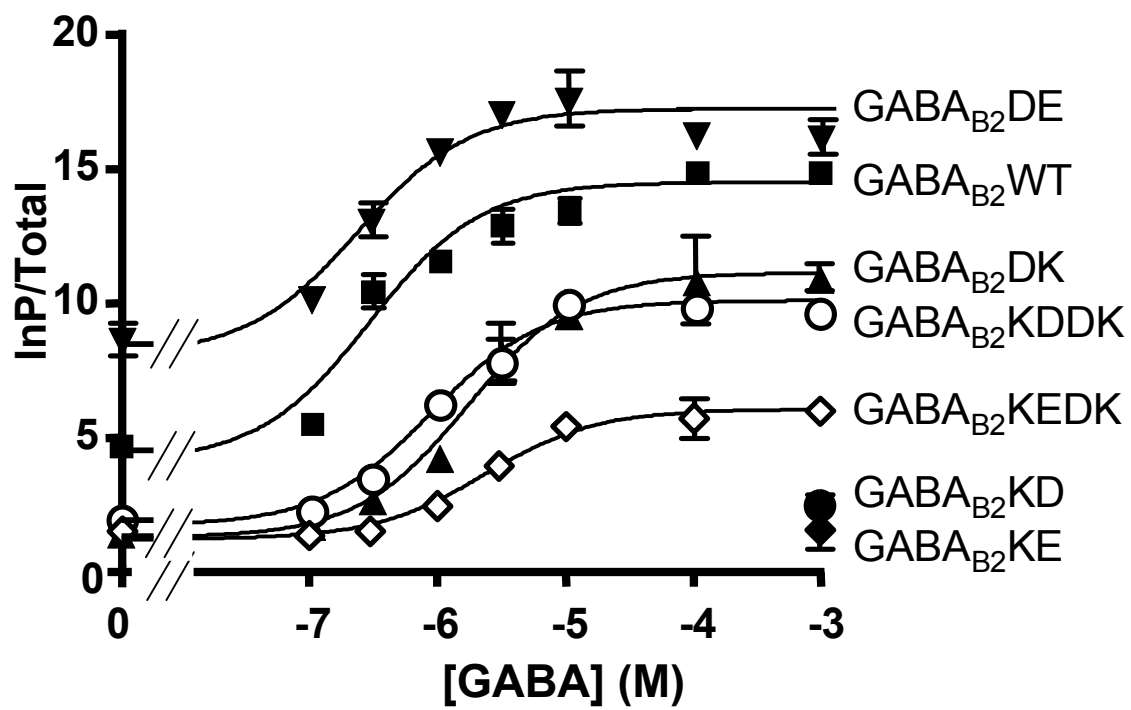


Fig.7

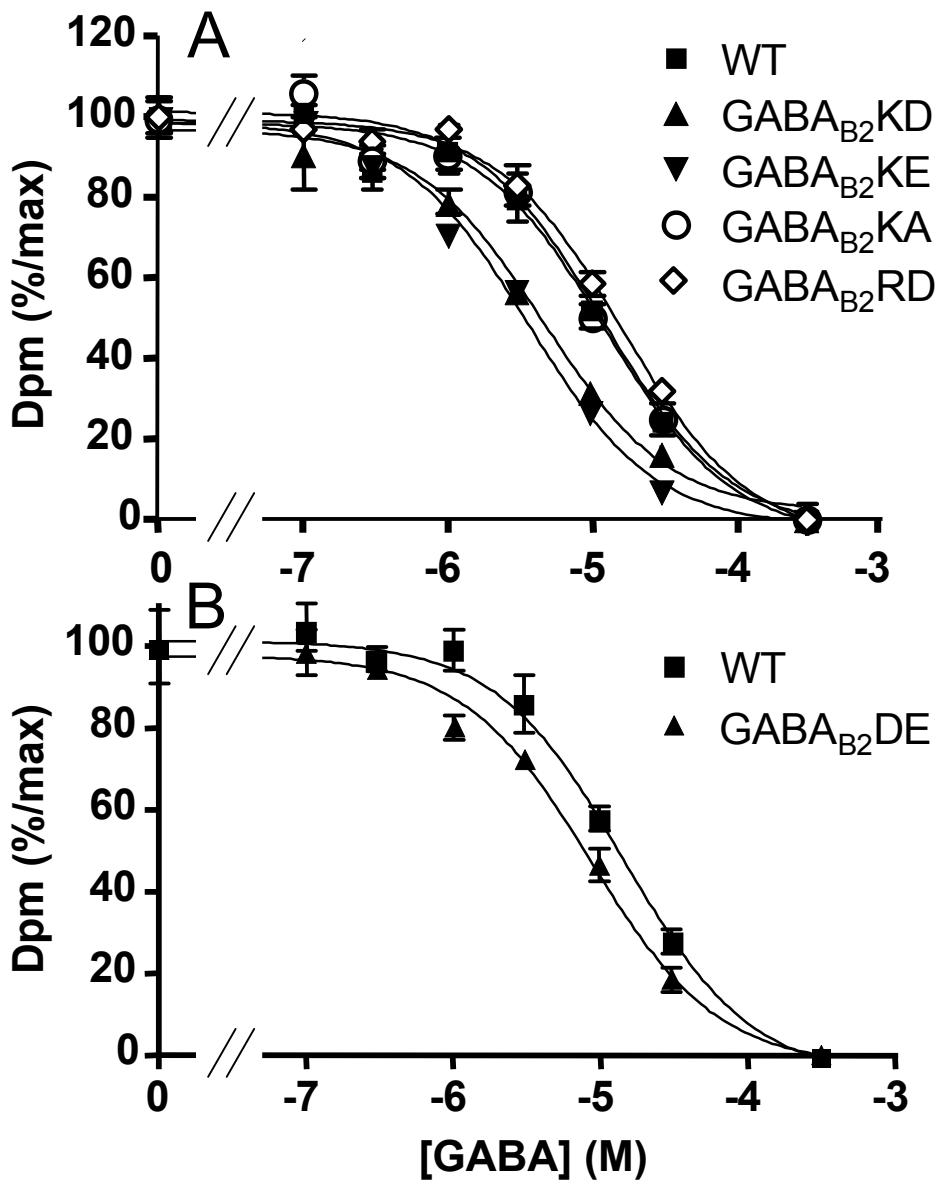


Fig.8

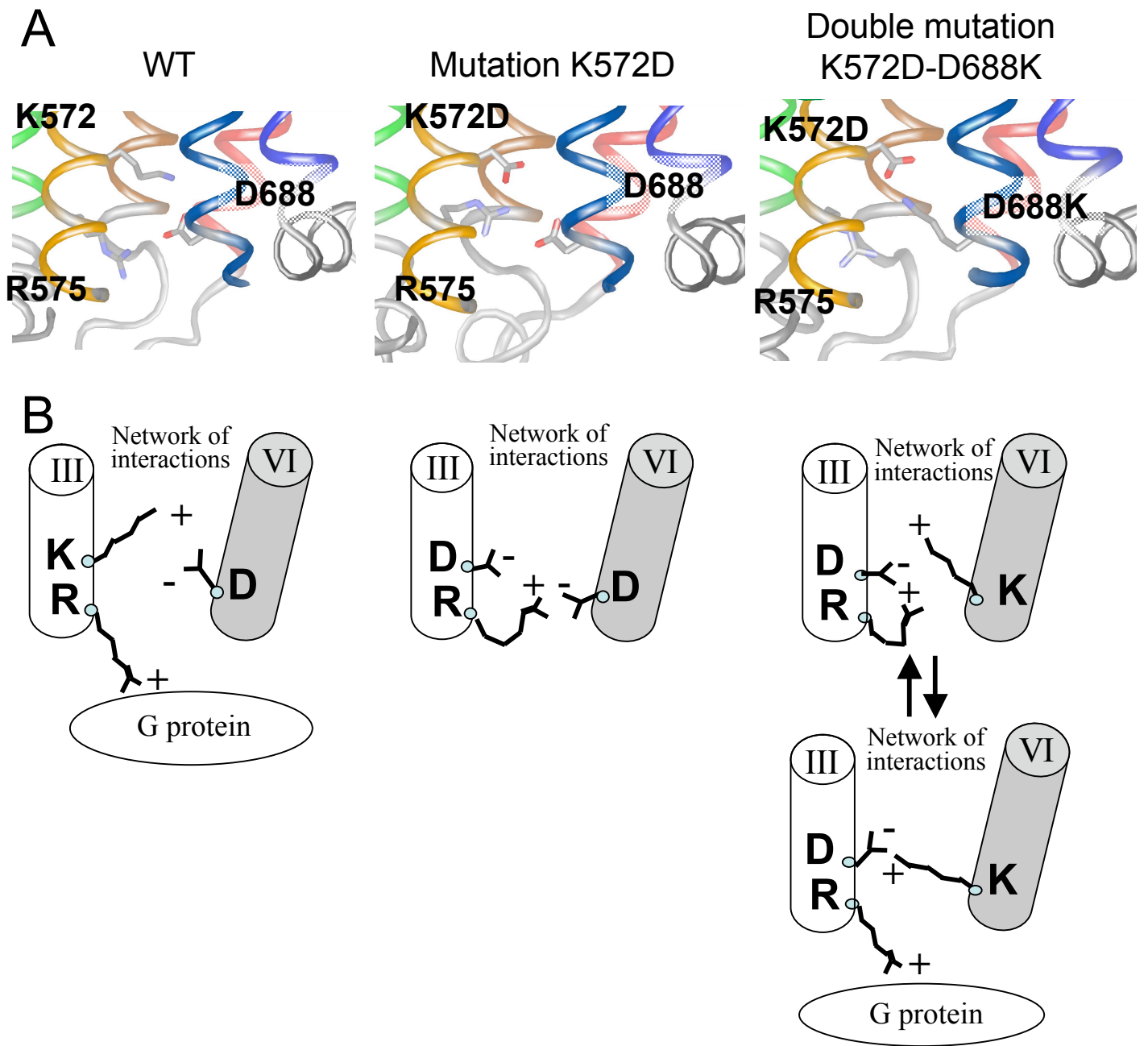


Fig.9